MINERALOGICAL MAGAZINE

VOLUME 40 NUMBER 315 SEPTEMBER 1976

Petrogenesis of migmatites in the Huntly–Portsoy area, north-east Scotland

J. R. ASHWORTH

Department of Physics, University of Essex, Wivenhoe Park, Colchester[1]

SUMMARY. Migmatites are described from the Sillimanite–potash-feldspar Zone of the aureole around the Newer Basic suite of synorogenic intrusions. The lowest-grade migmatites are trondhjemitoid (characterized by the assemblage quartz–plagioclase–biotite) or muscovite–granitoid (quartz–plagioclase–potash-feldspar–muscovite–sillimanite–biotite). With increasing grade, a transition occurs to cordierite–granitoid assemblages (quartz–plagioclase–potash-feldspar–cordierite–garnet–sillimanite–biotite), which persist to the highest grades observed, where there are also noritoid migmatites (quartz–plagioclase–orthopyroxene–cordierite–biotite). The trondhjemitoids are texturally simple because the minerals did not undergo dehydration reactions. Textural immaturity and consistently cotectic modal compositions indicate that their leucosomes originated as melts. Scatter of plagioclase compositions suggests that the partial melting occurred in small closed systems. The other migmatites have more fusible compositions, so it is deduced that they also underwent partial melting. Retrograde reaction textures are used to infer the sequence of reactions, involving muscovite and biotite, by which melting proceeded during prograde evolution. Whereas the fugacity of water probably varied among spatially associated trondhjemitoid leucosomes, in the muscovite-granitoids it was constrained to an approximately constant value, at given pressure and temperature, by the buffering effect of the mineral assemblage.

IT is widely believed that large-scale occurrences of migmatites in rocks of high metamorphic grade are due to partial melting *in situ* (e.g. Winkler, 1967; Turner, 1968), but there are still only a few areas in which this hypothesis has been tested against evidence from the rocks themselves (Mehnert, 1968). The area around Huntly (Aberdeenshire) and Portsoy (Banffshire) is auspicious for this purpose because it contains a variety of migmatites in a small area that have suffered little subsequent change. The area was mapped by Read (1923) and is part of the 'sillimanite-overprinted' Dalradian terrain for which Chinner (1966) has already discussed the possibility of melting. The migmatites are confined to, and abundant in, the Sillimanite–potash-feldspar Zone, which represents the highest metamorphic grade of the area (Ashworth, 1975). This zone is the inner part of the thermal aureole of the Newer Basic igneous masses. These include gabbros, norites, and allied rocks, which were

[1] Present address: Dept. of Geological Sciences, University of Aston in Birmingham, Gosta Green, Birmingham B4 7ET.

intruded at a late stage in the regional metamorphism that accompanied the Caledonian orogeny, and have a Rb–Sr age of 501±17 Myr (Pankhurst, 1974). The metamorphic zones of the aureole and the migmatite localities are indicated in fig. 1. The scarcity of localities is due to poor exposure; pelites and semipelites of the Sillimanite–potash-feldspar Zone are usually migmatized.

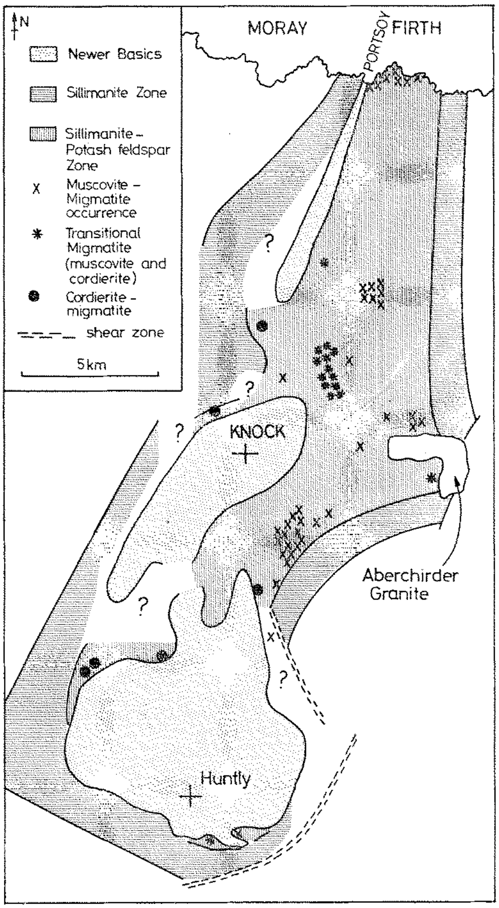

FIG. 1. Simplified petrological map of the Huntly–Portsoy area, showing migmatite localities in the metamorphic aureole around the Huntly, Knock, and Portsoy Newer Basic Masses. Bottom left-hand corner is at grid reference NJ 460360, top right-hand corner at 640690.

The migmatites are mostly of two kinds: *granitoid*, in which the leucosomes[1] contain essential potash feldspar and *trondhjemitoid* in which this feldspar is absent. Muscovite-granitoid migmatites occur in the lower-grade part of the Sillimanite–potash-feldspar Zone and typically have the assemblage quartz–plagioclase - potash - feldspar - muscovite - sillimanite–biotite. Trondhjemitoid migmatites also occur at this grade but in rocks lacking muscovite; they mostly have the simple composition quartz - plagioclase - biotite. These rocks are common on the coast but are rarely seen inland; they occur wherever muscovite-free semipelites are at the appropriate grade. Cordierite-granitoid migmatites shown on fig. 1 typically have the leucosome assemblage quartz–plagioclase–potash-feldspar - cordierite - garnet - sillimanite–biotite. They are the hornfelses of Read (1923), and the non-leucosomes are indeed hornfelsic. These granitoids persist in metasedimentary inclusions within the Newer Basic rocks where they occur along with the widely known cordierite-norites. The

[1] Terms used in this paper are modified after Mehnert (1968): Neosomes are rocks generated by migmatization, while palaeosomes are spatially associated unmodified lithologies. Leucosomes and melanosomes are leucocratic and melanocratic neosomes respectively. Leucosomes tend to occur in contact with complementary melanosomes. Mobilizates are segregations of mobile material while restites are the relatively immobile parts of the neosomes. Stromatic migmatites are layered and agmatites are breccia-like. Nebulites have macroscopically diffuse boundaries between leucosomes and melanosomes. Schlieren migmatites include streaks or irregular masses of palaeosome or melanosome while in schollen migmatites these inclusions are rounded.

latter are characterized by the assemblage quartz–plagioclase–orthopyroxene–cordierite–biotite; garnet is also often present but potash feldspar is absent. Read (1923) regarded these rocks as contaminated derivatives of the basic magma but Gribble (1970) has reinterpreted them as the products of partial melting of metasediments, and has presented strong evidence for partial melting as the origin of all the cordierite-norites of north-east Scotland (Gribble, 1968). Although most geologists would not call these rocks migmatites (Read, 1943), they are mentioned here as the culmination of the sequence of migmatization effects in the area, and are designated *noritoid* migmatites.

The structures of the trondhjemitoid and muscovite-granitoid migmatites are best seen in the coast section, where higher grades are unrepresented. They are predominantly stromatic, though large muscovite-granitoid leucosomes develop schlieren structure. Muscovite-free cordierite-granitoid migmatites are sometimes similarly stromatic, though the structure is harder to define because, in hand-specimen, leucosomes are more similar in colour to melanosomes, and both have textural complexities. Stromatic leucosomes here tend to be small, and transitions exist to small-scale agmatitic structure. Rocks carrying both muscovite and cordierite (muscovite-cordierite-granitoid grade), are best seen a few km north-east of the north end of the Knock Newer Basic Mass (fig. 1), on the upper parts of Culvie Hill and Corn Hill (around grid reference NJ 580548 and 579563 respectively). There is little or no exposure of rock *in situ*, but the regolithic boulder-fields are petrographically consistent to a degree that ensures that they are representative of local bedrock. These rocks are intensely migmatized, and are dominated by coarse, pale leucosome material, which contains schlieren and schollen of melanosome and palaeosome. Among the noritoids, stromatic types occur, but most have schollen structure—the 'xenolithic' appearance noted by Read (1923).

The trondhjemitoid migmatites

Although scarce, these will be treated first because they are the simplest to interpret. Similar migmatites occur elsewhere, often on a larger scale, and sometimes in association with granitoids or other types (e.g. Read, 1927, 1952; Misch, 1968; Kalsbeek, 1970). They are prominent in the area studied very thoroughly by Mehnert (1953 to 1963). The samples studied in detail all come from the coast section.

Qualitative petrography. These migmatites are dominated by the three minerals quartz, plagioclase, and biotite. Biotite is red-brown, pleochroic to nearly colourless. Garnet is pink, and is no doubt almandine. Most rocks have accessory opaque minerals. Actinolite occurs in associated palaeosomes, and varies between colourless and distinctly green in thin-section, with extinction angles $\gamma : [001] = 17$ to $20°$. Cummingtonite also occurs; it shows lamellar twinning, and is paler than coexisting actinolite. The very fine-grained, altered orthoamphibole occasionally seen is presumably anthophyllite. Chlorite and muscovite are typically associated with cataclasis, and are regarded as late retrograde products associated with shear-zones. These two minerals also occur in pinite pseudomorphs after cordierite, which is scarce in these rocks and is more usually altered to yellow, nearly isotropic material. Zircon, apatite, and tourmaline are common accessories.

Leucosomes are coarser than associated non-leucosomes (fig. 2). Melanosomes occur adjacent to leucosomes, but are generally thin and poorly developed. As well as being enriched in biotite relative to the leucosomes, they are sometimes richer in either quartz or plagioclase, occasionally being virtually dimineralic (fig. 2b). A few are thin

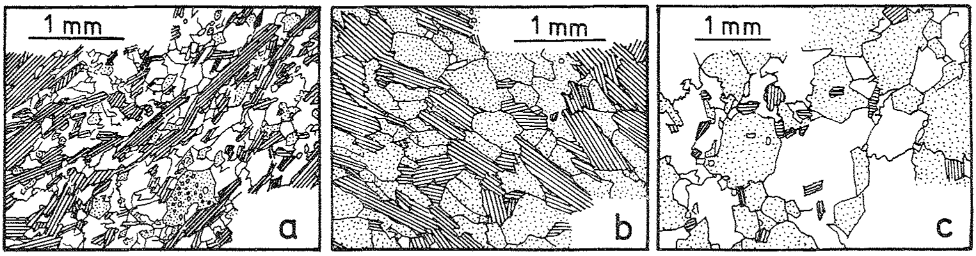

FIG. 2. Petrographic sketches of typical lithologies of the trondhjemitoid migmatite suite, as seen in thin section. Quartz shown blank, plagioclase stippled, biotite ruled. *a*; palaeosome. Slide 105767/1. *b*; melanosome. 105514/1. *c*; leucosome. 105514/2.

enough to be described as biotite selvedges. Melanosomes are characteristically coarser than adjacent palaeosomes. Leucosomes have sharp boundaries, but melanosomes frequently grade into palaeosomes. Often, a melanosome cannot be discerned at the edge of a leucosome, the latter being in contact with a lithology indistinguishable from local palaeosome. Because of the difficulty of distinguishing melanosome from palaeosome in the field, and rapid spatial variations in the amount of leucosome, the proportions of the three types of body cannot be reliably estimated.

Textural description. Qualitatively, the leucosomes appear strikingly less well annealed than the other bodies. The work of Kretz (1969) provides a method of quantifying this effect. The rock is examined for departure from a random distribution of grain contacts. Departure from randomness will be in one of two senses: a *regular* distribution is one in which boundaries between grains of *different* minerals are more frequent than would be expected at random, given the over-all frequency of occurrence of each mineral; an *aggregate* distribution is one in which boundaries between grains of the same mineral are preferred, so that the grains tend towards an arrangement of monomineralic clusters. Of the approaches discussed by Kretz (1969), the line-transect method was chosen on grounds of convenience and interpretative simplicity. The sampling line (Kretz, 1969, fig. 6) was laid out with a point-counter stage. Care was taken to avoid rocks showing late deformational features (subgrains, fractures), which could confuse the results. By recording each grain as it is entered during the mechanical traverse, a sequence of contacts is obtained. The total number of contacts of each type is then used in constructing a contingency table, to which the χ^2 test is applied.[1] The results are summarized in Table I. All the rocks give χ^2 values

[1] The condition that the interval between the long traverses be greater than the maximum grain-size encountered (Kretz, 1969) was met. Following the point made by Flinn (1969, pp. 363–4), that the

TABLE I. *Results on textural relations of minerals, presented in the form of contingency tables*

Palaeosome 105508	P	B	Q	Total
P	20	76	109	205
	40	67	98	
B	63	44	193	300
	59	*98*	143	
Q	114	207	174	495
	97	162	*235*	
Total	197	327	476	1000
			$\chi^2 = 92{\cdot}05$	

Palaeosome 105514/1	P	B	Q	Total
P	43	152	101	296
	84	123	89	
B	134	138	129	401
	114	*167*	120	
Q	107	127	69	303
	86	126	*91*	
Total	284	417	299	1000
			$\chi^2 = 48{\cdot}04$	

Palaeosome 105766/1	P	B	Q	Total
P	12	69	60	141
	20	57	*64*	
B	57	77	236	370
	52	*150*	168	
Q	72	258	159	489
	69	198	*223*	
Total	141	404	455	1000
			$\chi^2 = 105{\cdot}31$	

Palaeosome 105768/1	P	B	Q	Total
P	12	41	92	145
	20	*50*	75	
B	39	70	206	315
	43	*108*	163	
Q	86	234	220	540
	74	186	*280*	
Total	137	345	518	1000
			$\chi^2 = 58{\cdot}18$	

Leucosome 105514/2	P	B	Q	Total
P	274	69	209	552
	298	*70*	184	
B	60	25	21	106
	57	14	*35*	
Q	205	33	104	342
	186	*44*	*114*	
Total	539	127	334	1000
			$\chi^2 = 26{\cdot}73$	

Leucosome 105515	P	B	Q	Total
P	150	66	203	419
	179	66	174	
B	56	24	61	141
	60	22	58	
Q	222	68	150	440
	188	*70*	*182*	
Total	428	158	414	1000
			$\chi^2 = 22{\cdot}12$	

Leucosome 105778	P	B	Q	Tota
P	230	60	212	502
	257	*64*	181	
B	47	22	43	112
	57	14	40	
Q	235	45	106	386
	198	*49*	*139*	
Total	512	127	361	1000
			$\chi^2 = 29{\cdot}97$	

Leucosome 105798	P	B	Q	Total
P	143	46	214	403
	165	*59*	179	
B	41	44	49	134
	55	20	*60*	
Q	225	56	182	463
	189	*68*	*206*	
Total	409	146	445	1000
			$\chi^2 = 59{\cdot}62$	

Leucosome 105799	P	B	Q	Total
P	166	87	175	428
	189	85	155	
B	81	30	59	170
	75	*34*	*62*	
Q	197	82	131	410
	181	81	*149*	
Total	444	199	365	1008
			$\chi^2 = 9{\cdot}90$	

P = plagioclase, B = biotite, Q = quartz+accessories. The cells in the column for a particular mineral show the number of contacts where that mineral was entered from the respective row minerals. Expected frequency is tabulated below observed in each cell. Expected frequencies greater than observed are distinguished by italics. χ^2 values for departure from randomness at various significance levels are: 95 % significance level, 9·49; 99 %, 13·28; and 99·9 %, 18·47.

strongly indicating departure from randomness. *Palaeosomes* show a simpler pattern than leucosomes; they have strongly *regular* distributions. Three leucosomes have

χ^2 analysis procedure can be biased by sample size, the latter was standardized at 1000 contacts. Even with a line layout that avoided intersection of one grain by more than one long traverse, it was found that the intricacy of contacts was sometimes such that it was impossible to avoid encountering contacts previously crossed on the same traverse. With care, it is possible to identify these 'recurrences'. It was found that in palaeosomes 10·0±0·5 % of boundaries crossed were recurrences, and in leucosomes 11 to 19 %, this higher range being no doubt due to their less mature textures. Recurrences were, of course, excluded from the data used for analysis. Homogeneity tests (Kretz, 1969) were not performed, on account of their apparent irrelevance (Flinn, 1969). Accessories were grouped with quartz to avoid the occurrence of cells with expected frequencies less than 5 (Flinn, 1969, p. 363).

regular distributions with respect to quartz and plagioclase, but aggregate with respect to biotite; the others are regular for all minerals. *Regularity is less strong in leucosomes* than in palaeosomes. Fig. 3 illustrates the distinction between the two classes of body.

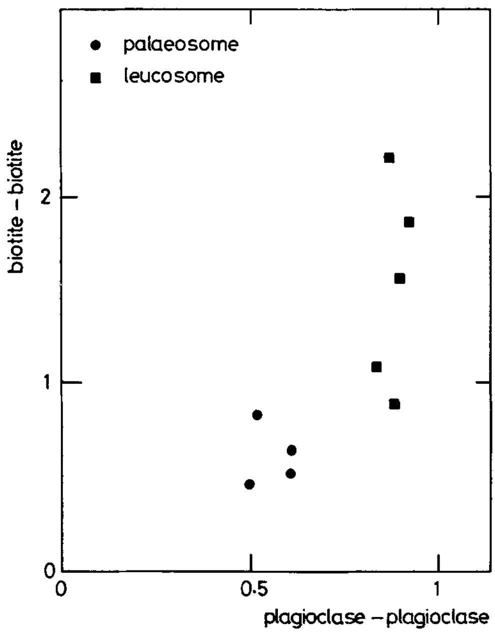

FIG. 3. Graphical illustration of the textural distinction between leucosomes and palaeosomes, using the relative frequency with which plagioclase is in contact with another grain of plagioclase, and the corresponding frequency of biotite–biotite contacts. The values plotted are the ratios between the observed frequency and the frequency expected on a random model, as listed in Table I. The palaeosomes have the more pronounced tendency to give observed/expected ratios less than unity, indicating a 'regular' distribution of grain contacts.

Interpretation of textures. Metamorphic annealing is believed to produce regular distributions (Flinn, 1969). The above results thus confirm that the leucosomes show less advanced effects of metamorphic annealing than do the palaeosomes. This indicates a less mature degree of solid-state evolution; their *textural immaturity* implies that the leucosomes formed by a process of primary crystal growth at a relatively late stage of the metamorphism of the area. This rules out an origin depending on textural equilibrium (DeVore, 1956). The results also contrast strongly with the textural evidence adduced by Loberg (1963) in proposing that leucosomes of similar composition can arise through solid-state reactions between phases; moreover, in the present simple assemblages there is no evidence for any such reaction. The observations suggest that the leucosomes crystallized from a fluid. Furthermore, the observation that melanosomes are texturally allied to palaeosomes rather than leucosomes (fig. 2) is consistent with the proposition that they represent the solid residua from which the fluid segregated.

Modal analysis and plagioclase compositions. The simple textures and mineralogy of the trondhjemitoids lead to simple modal compositions, which are easily estimated by point-counter. Point-intervals were chosen and errors estimated according to the method of Van der Plas and Tobi, 1965. The results are given in Table II. The ternary diagram (fig. 4) illustrates the low biotite-content of the leucosomes, and also that they tend to a consistent ratio of quartz to plagioclase.

In 14 leucosomes, 11 palaeosomes, and 4 unambiguously classifiable melanosomes, *plagioclase compositions* were estimated from the refractive index α' in cleavage flakes.[1] Repeatability experiments together with other considerations (Deer *et al.*,

[1] P. F. Kerr, 1959, *Optical Mineralogy*, 3rd edn., fig. 13–46, p. 273. New York (McGraw-Hill).

1963, pp. 129–32) lead to estimated accuracy of ±2 % An. Variation outside this likely error was sought in leucosomes, where zoning is often petrographically obvious. The refractive-index observations indicate the following approximate ranges of An %: 23 to 32 (leucosome 105509); 26 to 30 (105514); 27 to 32 (105523); 26 to 37 (105768); 16 to 30 (105770); 16 to 25 (105772); 23 to 25 (105778), and 35 to 39 (105798). The

TABLE II. *Modal analyses of trondhjemitoid migmatites*

Rock/slide number*		508	509/1	509/2	509/3	514/1	514/1	514/1	514/2	517/1	523	523/1
Type of body†		P	P	M	L	L	P	M	L	L	P	L
Estimated volume percentage	quartz	59·4	59·3	66·7	29·7	35·8	24·4	3·0	32·8	41·9	59·4	44·2
	plagioclase	20·5	17·2	11·2	56·7	58·4	39·6	44·0	61·6	42·4	19·1	54·6
	biotite	18·9	22·1	21·2	13·6	5·8	35·3	53·0	5·7	14·8	20·3	1·3
	other	1·2	1·4	0·8	—	—	0·6	—	—	1·0	1·4	—
Estimated standard deviation	quartz	1·6	1·6	3·1	3·7	4·2	1·8	0·7	3·5	3·5	1·9	5·6
	plagioclase	1·3	1·2	2·0	4·0	4·3	2·2	2·2	3·5	3·5	1·6	5·7
	biotite+others	1·3	1·3	2·6	2·8	2·0	2·1	2·2	1·5	2·5	1·7	1·3
Number of points		1000	1000	240	155	137	524	500	177	203	622	77
Point interval mm		0·3	0·3	0·7	1·7	0·7	0·3	0·3	1·7	1·7	0·3	1·7

Rock/slide number*		523/1	531	539/2	753	766	766/1	766/1	767/1	768/1	768/2	772/2
Type of body†		M	L	P	L	L	M	P	P	L	P	L
Estimated volume percentage	quartz	60·3	39·2	25·3	38·1	38·9	45·4	52·3	41·3	37·1	51·8	38·1
	plagioclase	2·0	50·9	27·8	61·2	54·1	13·4	15·0	16·0	53·1	13·6	53·2
	biotite	35·6	5·9	42·0	—	6·2	40·3	30·8	36·5	9·9	34·1	8·5
	actinolite	—	—	—	—	—	—	—	4·9	—	—	—
	other	2·0	4·1‡	4·8§	0·7	0·7	0·8	2·0	1·3	—	0·5	0·2
Estimated standard deviation	quartz	1·5	2·9	1·5	4·0	4·1	4·8	2·5	1·6	3·5	1·6	2·3
	plagioclase	0·4	3·0	1·6	4·0	4·1	3·3	1·8	1·2	3·6	1·1	2·4
	biotite+others	1·5	1·8	1·8	—	2·0	4·7	2·3	1·6	2·2	1·5	1·3
Number of points		1029	271	818	147	144	119	406	1000	181	1000	467
Point interval mm		0·3	1·7	0·7	1·7	1·7	0·7	0·3	0·3	1·0	0·3	1·0

Rock/slide number*		773	774/1	778/1	779	780	798	798	798	799/2	811
Type of body†		P	L	L	P	M	L	M	P	L	P
Estimated volume percentage	quartz	34·9	37·7	42·1	34·0	33·7	47·8	41·3	50·9	39·5	43·2
	plagioclase	25·3	46·7	52·0	23·4	23·1	47·1	9·2	19·9	51·9	14·0
	biotite	37·1	15·3	5·3	38·0	40·7	5·2	49·2	28·4	6·5	35·9
	garnet	—	—	—	3·7	1·7	—	—	—	—	—
	actinolite	—	—	—	—	—	—	—	—	—	5·9
	other	2·7	0·4	0·7	0·9	0·8	—	0·3	0·8	2·2	1·1
Estimated standard deviation	quartz	1·5	3·3	4·0	1·5	1·5	3·1	2·8	2·7	3·5	1·6
	plagioclase	1·4	3·4	4·1	1·4	1·3	3·1	1·6	2·2	3·7	1·2
	biotite+others	1·5	2·4	1·7	1·6	1·6	1·2	2·9	2·4	2·0	1·6
Number of points		1000	223	152	1000	1000	270	317	377	185	1007
Point interval mm		0·3	1·0	1·7	0·3	0·3	1·7	0·3	0·3	1·7	0·3

* Prefixed 105. † L = leucosome, M = melanosome, P = palaeosome. ‡ Muscovite. § Largely pinite.

gross variations within a body indicate that equilibrium was violated. *Zoning*, observed petrographically in leucosome plagioclase, is almost always 'normal' (to lower An-content outwards). Large grains sometimes have confused, patchy zoning near their centres (cf. Mehnert, 1968, p. 260). In large leucosomes, coarse plagioclase often shows *idiomorphic* zone-boundaries. The boundary divides a normally zoned outer part from a central part with only very slight zoning. Only in one case was the phenomenon reported by Mehnert (1963), in which zoning is reverse up to the boundary, definitely observed; this rock is also anomalous, for the present area, in showing well-developed oscillatory zoning. The idiomorphic boundaries must represent some change in conditions during the growth of the plagioclase crystals, but more importantly for fundamental interpretation they indicate growth in a mechanically isotropic environment, which was presumably a fluid.

Fig. 5 shows that leucosome plagioclase compositions correlate closely with those in coexisting melanosomes, but not in adjacent palaeosomes. This result, and the failure of palaeosomes to lie on straight lines joining coexisting leucosomes and melanosomes in fig. 4, indicate that, in general, a palaeosome does not have the same bulk composition as an adjacent system that became migmatized.

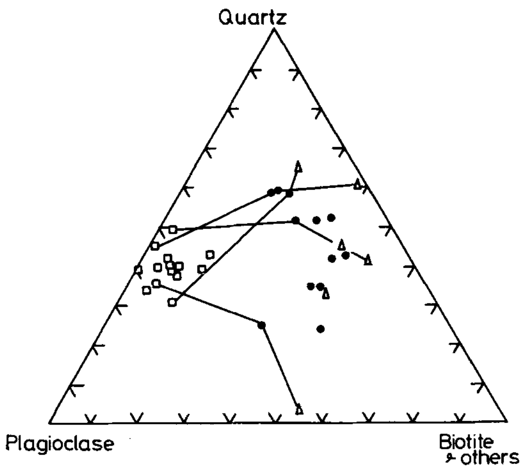

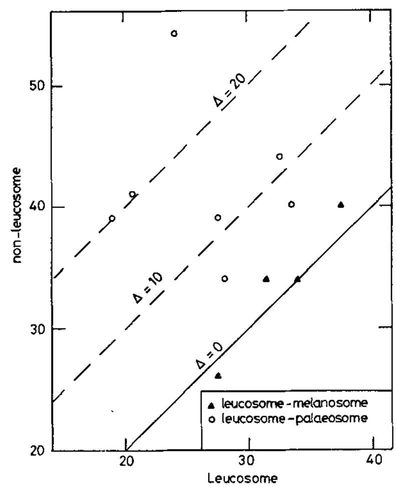

FIGS. 4 and 5: FIG. 4 (left). Graphical representation of modal analyses of the trondhjemitoids. Squares represent leucosomes, triangles melanosomes, and circles palaeosomes. Tie-lines indicate spatially associated bodies. FIG. 5 (right). Estimated plagioclase compositions (An percent) for spatial associations between trondhjemitoid leucosomes and non-leucosomes. Δ is the amount by which the non-leucosome plagioclase has higher anorthite content than does the associated leucosome plagioclase. Leucosome values plotted are the mid-points of observed compositional ranges.

In non-leucosomes, zoning was rarely detected. The observed range of plagioclase composition in palaeosomes as a whole is An_{27} to An_{54}, while in leucosomes and melanosomes taken together the range is An_{16} to An_{39}. Thus the neosomes occupy a more sodic compositional range than the spatially associated palaeosomes, but the ranges overlap.

Petrogenetic interpretation. The idiomorphic zone-boundaries confirm that the textural results should be interpreted in terms of leucosome crystallization from a fluid at a relatively late stage in the metamorphic history of the area. That the mineral chemistry was controlled within small systems suggests that the fluid was locally generated. In this case it cannot have been an aqueous gas phase, since no dehydration reactions occurred that could produce segregable quantities of this phase. Combining the modal analysis and plagioclase composition data gives excellent agreement with experimentally determined cotectic compositions (fig. 6).[1] This confirms that the fluid was a *melt.*

[1] Plagioclase composition estimates are by refractive index or by extinction angles in the section |*a*

The correlation between leucosome and melanosome plagioclase compositions (fig. 5) is to be expected if melting occurred in small closed systems (cf. Mehnert, 1962). Control of composition within small systems allowed a wide range of plagioclase composition to persist among leucosomes. The tendency of palaeosomes to have more calcic plagioclase than adjacent neosomes is not a differentiation effect; the palaeosomes were more calcic from the outset, and this inhibited migmatization.

As well as the small-system chemical relations, the small size ($\lesssim$ 1 m) and stromatic geometry of leucosomes render it implausible to suggest that the melt was mechanically introduced from outside. Moreover, no source for such a magma could be found; no trondhjemitic intrusions are known in the area. A different unknown magma would have to be invoked for the intimately spatially associated muscovite-granitoids. These considerations lead to the conclusion that the melt was locally derived. The process was that usually called partial melting *in situ*.

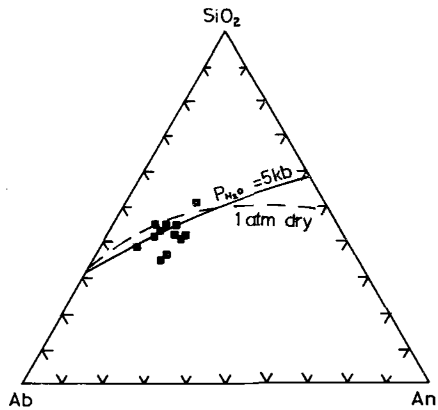

FIG. 6. Trondhjemitoid leucosome compositional data compared with the experimentally determined cotectics in the system Ab–An–SiO_2–H_2O (after Yoder, 1967).

Kalsbeek (1970) argues that mineral dehydration reactions producing potash feldspar (cf. below) would be expected in this case, but it is shown below that biotite assemblages require more severe conditions than do muscovite-bearing ones to initiate their dehydration. There is, in general, a wider temperature interval for biotite stability on the liquidus than for muscovite, at a given pressure (Brown and Fyfe, 1970).

The plagioclase composition data rule out imposition of mineral compositions by metasomatism, but do not rule out minor, relatively inefficient metasomatic interactions. However, it is noteworthy that any such metasomatism failed to eliminate zoning, and failed to cause melting of some palaeosomes having plagioclase as sodic as that in nearby leucosomes. The survival of the zoning rules out any interpretation of the lack of differentiation between leucosome and melanosome plagioclase in terms of thorough retrograde reaction between these bodies (cf. Mehnert, 1962). The scatter of leucosome plagioclase compositions, among rocks with virtually identical pressure–temperature histories, indicates that at least one chemical activity, other than those of the components of plagioclase, was variable from rock to rock. The simple mineralogy limits the possibilities for such variation, and the most reasonable interpretation is that the variable was the fugacity of water, f_{H_2O}. This interpretation implies that melting occurred under water-undersaturated conditions. Rocks with plagioclase more sodic than An_{39} incipiently melted, but only in those with initially high f_{H_2O} was

(Deer *et al.*, 1963, fig. 55). The difference between weight per cent (plotted by Yoder, 1967) and volume per cent (modal analysis) is negligible. Paucity of biotite in leucosomes suggests that its presence will displace the cotectic only minimally (cf. Winkler, 1967, pp. 208–16).

enough melt formed for segregation to form neosomes. All the melts were climactically water-undersaturated. Water-undersaturation is accompanied by marked bivariance of the melting interval, even for a eutectic composition (Brown, 1970). This may explain the paucity of differentiation between leucosome and melanosome plagioclase compositions, as well as the slightness of central zoning in the plagioclase grains that have idiomorphic zone-boundaries; the melt may crystallize silicates of almost constant composition while it evolves to higher water-contents. Only when it attains the water-saturated cotectic is it constrained to follow the experimentally familiar trend of fractional crystallization. Alternatively, the zone-boundaries could be interpreted in terms of dissociation of melt from melanosome (cf. Mehnert, 1963), though in the Huntly–Portsoy area it is extremely unlikely that melts moved far enough to experience a virtual discontinuity in pressure–temperature conditions.

In summary, the trondhjemitoid migmatites are interpreted in terms of partial melting in small closed systems. The melt segregated into leucosomes with dimensions up to ~ 1 m, but did not further coalesce or migrate, or interact discernibly by diffusion with adjacent systems. Melanosomes are restites corresponding to adjacent mobilizate leucosomes. Presumably, some lithologies that cannot unambiguously be classified as melanosomes are also restitic. Availability of water controlled the extent of melting, and absorption of water into the melt presumably hindered diffusion.

The interpretation of a Dalradian trondhjemitoid migmatite suite without appeal to either magmatic injection or metasomatism may be of interest if a reinvestigation is attempted of similar occurrences, such as that in Cromar (Read, 1927). The present area is similar in many respects to the Black Forest area of Mehnert (1953 to 1968).

It is apparent that the interpretability of the Huntly–Portsoy trondhjemitoids is a fortunate result of the general lack of postmigmatization deformation or metamorphism, which would have destroyed the all-important textural relations. The other migmatites of the area can now be interpreted by analogy with the trondhjemitoids.

The muscovite-granitoid migmatites

Qualitative petrography. The characteristic assemblage is quartz–plagioclase–microcline–muscovite–sillimanite–biotite, often with garnet in addition. Some calcareous palaeosomes have the assemblage quartz–plagioclase–microcline–actinolite–biotite. Opaque minerals are generally scarce, but pyrite was identified in material polished for electron-probe work, and fine dark material, which is often associated with micas, is probably graphite. Biotite and garnet are like those of the trondhjemitoids. Sillimanite is fine-grained and acicular, i.e. fibrolitic. Muscovite is often coarse and discordant to the biotite foliation that is prominent in non-leucosomes (fig. 7). Zircon, apatite, and tourmaline are common accessories, tourmaline being particularly prominent in some coarse leucosomes.

Fig. 7 illustrates typical lithologies. Petrography is more complex than in the trondhjemitoids. One reason is greater variability in modal composition. Not only are schlieren structures fairly frequent, tending to obscure the boundaries of bodies, but the biotite-poor (psammitic) composition of some of the metasediments increases the difficulty of distinguishing between bodies on compositional grounds; in these rocks the term melanosome is often inappropriate, so the term *restite* will be used instead. Leucosomes generally remain distinct by being coarser than restites and palaeosomes. Restite textures are similar to those of palaeosomes. Leucosomes, on the other hand, often show advanced *reaction textures* culminating in the complete replacement of microcline by muscovite, quartz, and myrmekite (Ashworth, 1972). Fibrolite in these rocks is often surrounded by muscovite. The muscovite in the reaction textures has

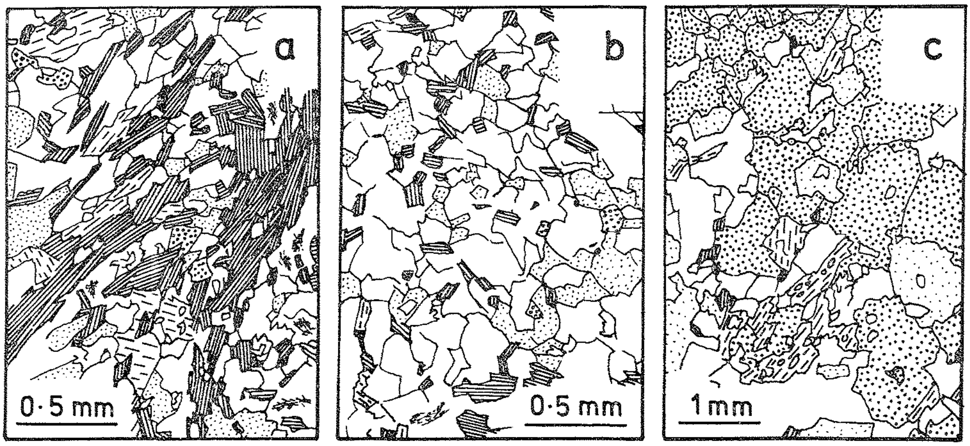

FIG. 7. Petrographic sketches of typical lithologies of the muscovite-granitoid migmatites of the coast section. Quartz shown blank, plagioclase ornamented by light stippling, microcline heavy stippling, muscovite light ruling, biotite heavy ruling; fibrolite clots indicated schematically. *a*; semipelite, probably restitic. Slide 105497. *b*; psammite, probably restitic. 105784/1. *c*; leucosome. 105496/1.

the same composition as other muscovite in the rock; all the muscovite, in both restites and leucosomes, belongs to the primary assemblage (Ashworth, 1975). The textures in leucosomes represent early retrograde replacement of the pair microcline–sillimanite by the hydrous equivalent. The reaction is that corresponding to retrogression at the Sillimanite–potash-feldspar 'isograd' (Ashworth, 1972, 1975):

$$\text{potash feldspar} + \text{sillimanite} + \text{fluid} \rightarrow \text{muscovite} + \text{quartz} + \text{plagioclase}. \quad (1)$$

Modal analysis and plagioclase compositions. Table III shows modal analyses of coastal rocks, and of schlieren-migmatites from the higher-grade locality called Starmires quarry (grid reference 587559). Fig. 8 shows that the muscovite-granitoid leucosomes are much less closely grouped compositionally than are the trondhjemitoids (fig. 4), and that this is particularly so for the schlieren-migmatites. The latter point suggests that the scatter is partly due to restitic 'contamination'. There is a hint of this even in the trondhjemitoids, where the variable biotite-content of leucosomes (fig. 4) may reflect mechanical incorporation of biotitic micro-schlieren (cf. Mehnert, 1963, especially Abb. 7), particularly as biotite tends to have aggregate textural relations (Table 1). Therefore, in fig. 9, schlieren-migmatites are excluded altogether, and among the remaining (stromatic) leucosomes those with more than 5 % of minerals

TABLE III. *Modal analyses of muscovite-granitoid migmatites. The first 28 are typical rocks of the coast section; the last 9 are schlieren-migmatites from Starmires quarry*

Rock/slide number*		496/1	496/2	496/2	496/4	497	502	519/2	520	534	535	536	751	752
Type of body†		L	L	R	L	R	R	L	L	L	R	R	L	R
Estimated volume percentage	quartz	52·1	43·3	69·6	34·9	30·5	62·4	37·6	27·3	39·4	55·7	60·8	34·5	49·6
	plagioclase	39·6	29·9	12·0	15·1	13·7	14·1	57·9	31·9	10·2	13·4	12·9	53·6	42·9
	microcline	—	17·9	2·4	45·2	4·6	—	—	37·1	46·4	0·9	10·9	2·7	3·8
	muscovite	0·8	1·5	3·2	3·2	4·7	7·4	3·0	0·7	1·6	1·7	3·5	0·9	0·8
	biotite	5·9	7·5	11·2	1·6	41·5	15·6	1·5	3·2	2·4	22·1	10·7	7·3	3·0
	sillimanite	0·8	—	—	—	2·5	0·3	—	—	—	4·3	0·4	0·9	—
	other	0·8	—	1·6	—	2·6	0·3	—	—	—	1·9	0·6	—	—
Estimated standard deviation	quartz	4·6	6·0	4·0	4·2	1·5	3·7	4·1	3·6	4·3	1·6	1·6	3·2	4·3
	plagioclase	4·4	5·5	2·8	3·1	1·1	1·9	4·2	3·7	2·7	1·1	1·1	3·3	4·2
	microcline	—	4·8	—	4·4	0·6	—	—	3·8	4·4	—	1·0	1·0	1·8
	rest	2·5	3·5	3·3	2·0	1·6	2·4	1·9	1·8	1·9	1·4	1·2	1·9	1·8
Number of points		119	67	125	126	1000	324	133	154	127	1000	1000	220	133
Point interval mm		1·0	1·7	0·7	1·7	0·3	1·0	1·7	1·7	1·7	0·3	0·7	1·7	1·7

Rock/slide number*		776/1	776/2	783/1	783/2	784/1	786/1	788	822/1	823	824/1	825	884/2
Type of body†		L	L	L	R	R	L	L	L	L	L	L	R
Estimated volume percentage	quartz	39·9	43·0	50·3	77·1	67·3	37·6	53·6	24·1	36·4	29·2	29·1	42·6
	plagioclase	36·1	43·0	42·4	14·3	11·1	39·7	22·0	44·6	36·4	31·5	33·8	10·0
	microcline	14·7	—	—	—	0·9	18·4	6·6	28·1	22·4	35·4	33·1	0·1
	muscovite	5·5	0·9	0·3	—	2·4	3·6	3·0	2·7	2·9	2·8	2·7	1·5
	biotite	3·0	5·6	6·9	8·0	17·6	0·7	14·9	0·4	1·2	1·1	0·7	28·3
	sillimanite	0·8	7·5	—	—	0·4	—	—	—	—	—	—	3·7
	other	—	—	—	0·6	0·3	—	—	—	0·6	—	0·7	1·3
Estimated standard deviation	quartz	3·2	4·9	2·9	1·4	1·5	4·0	3·9	2·8	3·7	3·4	3·7	1·6
	plagioclase	3·1	4·9	2·9	1·1	1·0	4·1	3·3	3·3	3·7	3·4	3·9	0·9
	microcline	2·2	—	—	—	—	3·3	1·7	2·9	3·3	3·7	3·8	—
	rest	1·8	3·5	1·4	0·9	1·3	1·8	3·0	1·0	1·6	1·6	1·8	1·5
Number of points		236	107	290	1000	1000	141	168	224	170	178	148	1000
Point interval mm		1·0	1·7	1·0	0·3	0·3	1·7	1·7	1·7	1·7	1·7	1·7	0·3

Rock/slide number*		630	631	633/2	581/1	581/1	581/2	581/2	582/1	582/2	582/2	583	723
Type of body†		L	L	L	L	R	L	R	L	L	R	L	L
Estimated volume percentage	quartz	32·8	35·7	34·4	26·0	0·5	45·9	9·3	53·3	54·1	55·4	45·9	62·0
	plagioclase	21·7	23·9	20·2	52·8	53·4	38·4	48·8	18·6	33·3	30·6	19·3	8·6
	microcline	37·0	23·2	40·5	—	—	—	—	1·8	—	—	6·7	26·4
	muscovite	6·3	12·1	4·3	2·3	0·5	4·8	2·5	12·6	0·9	—	10·4	2·5
	biotite	2·1	3·0	0·6	19·1	45·0	9·7	39·5	12·0	11·7	13·5	14·7	0·6
	sillimanite	—	2·0	—	—	—	0·8	—	1·2	—	—	2·2	—
	other	—	—	—	—	0·5	—	—	0·6	—	0·6	0·7	—
Estimated standard deviation	quartz	3·3	2·7	3·8	2·9	—	4·7	2·8	3·9	4·8	2·2	4·5	3·8
	plagioclase	2·9	2·5	3·2	3·4	3·6	4·6	4·7	3·0	4·6	2·0	3·4	2·2
	microcline	3·4	2·5	3·9	—	—	—	—	—	—	—	2·0	3·4
	rest	1·9	2·2	1·7	2·8	3·6	3·4	4·7	3·4	3·1	1·5	3·9	1·3
Number of points		189	297	163	220	191	124	119	167	111	533	135	163
Point interval mm		1·7	1·7	1·7	1·2	0·7	1·7	0·7	1·7	1·3	0·7	1·7	2·3

* Prefixed 105, except for 630, 631, and 633, which are prefixed 113.
† L = leucosome, R = restite.

other than quartz and feldspars are distinguished. Even so, there remains a great deal of scatter, and no convincing agreement with the cotectic curves.

Electron-probe analytical data for muscovite and plagioclase in neosomes are summarized elsewhere (Ashworth, 1975). Some microclines were probed, but the results are complicated by incipient perthitic exsolution (Ashworth, 1972). As in the trondhjemitoids, leucosome and restite *plagioclase compositions* correlate closely.

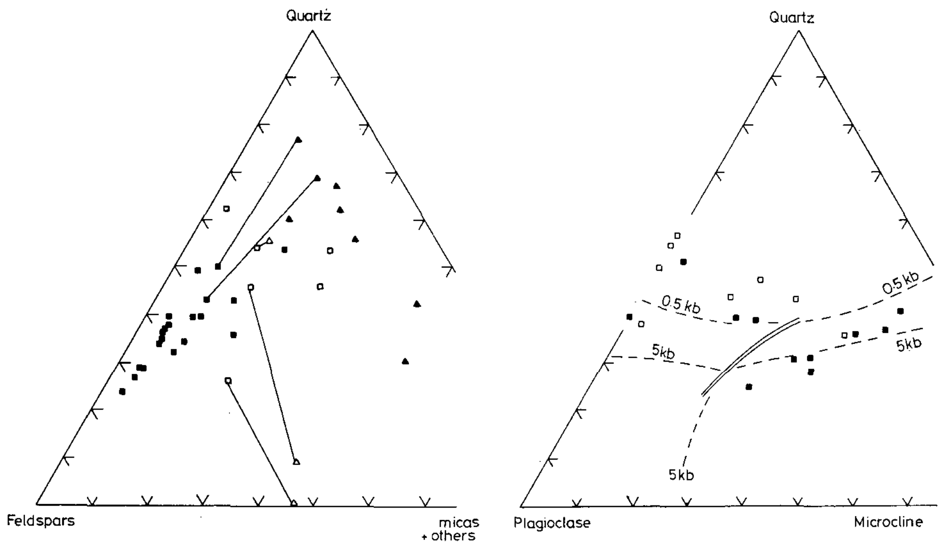

FIGS. 8 and 9: FIG. 8 (left). Graphical representation of modal analyses of the muscovite-granitoids. Squares represent leucosomes, triangles restites. Filled symbols represent rocks from the coast section, open symbols schlieren-migmatites from a slightly higher-grade locality (Starmires quarry). Tie-lines indicate spatial associations. FIG. 9 (right). Modal analyses of stromatic muscovite-granitoid leucosomes compared with experimentally determined cotectic relations after Luth *et al.* (1964). Pecked lines; cotectics. Double line; trace of the water-saturated minimum melting composition as a function of pressure from 0·5 to 10 kb. Open squares are used to distinguish those leucosomes containing more than 5 percent micas.

Mean An-contents of plagioclase from the electron-probe data are: rock 105497, leucosome 32·0, restite 31·4; 105502, leucosome 22·8, restite 24·2; 105535, leucosome 30·9, restite 30·9; 105785, leucosome 26·1, restite 24·0; and 105884, leucosome 31·5, restite 32·0. The electron-probe is much more accurate than the more indirect methods of composition estimation used in the trondhjemitoids. Accuracy is estimated as $\pm$ 0·2 mole % An under the conditions used. Variation of plagioclase An-content was detected in all the bodies studied from the muscovite-granitoid suite, as follows: 105497, leucosome 28·6–33·9, restite 28·4–32·4; 105499, leucosome 31·2–34·3; 105502, leucosome 21·7–23·7, restite 21·3–28·4; 105503, leucosome 26·2–29·4; 105519, leucosome 12·7–14·3; 105535, leucosome 29·1–31·8, restite 28·3–33·3; 105785/1, leucosome 19·3–32·4; 105785/2, leucosome 22·5–31·8, restite 22·1–32·6; 105785/3, leucosome 16·4–32·0; and 105884, leucosome 25·8–35·2, restite 27·8–35·8. Because of the small size of electron-probe specimens, these ranges should be regarded as minimum estimates. The small specimen-size ensured that leucosome and restite material was sampled at closely adjacent places in the same rock. There is no discernible differentiation effect.

Plagioclase zoning is not as striking petrographically as in the trondhjemitoids; idiomorphic boundaries are rare. Zoning was assessed by paired electron-probe analyses of points located respectively at centres and edges of sections through grains.[1] In leucosomes, 23 cases of normal zoning and 5 of reverse were found; in restites, 10 of reverse and 9 of normal. These data are insufficient to establish any significant difference between the leucosomes and the restites. Reverse zoning is always slight, ranging up to $An_{1.4}$ in leucosomes and $An_{3.9}$ in restites, whereas normal zoning was observed up to $An_{8.7}$ in leucosomes and $An_{9.8}$ in restites. Prevalence of normal zoning is attributed to continued reaction between restite and melt during cooling. Muscovite is also undifferentiated between leucosome and restite (Ashworth, 1975).

Comparison with the trondhjemitoids. The above data for the granitoids are inconclusive for the melting hypothesis. However, where trondhjemitoid melting occurs, the temperature must be above the water-saturated minimum for melting in rocks bearing potash feldspar as well as sodic plagioclase. The compositional range of plagioclase in the muscovite-granitoids is nearly the same as in the trondhjemitoids. Minimum melting temperatures should be markedly lowered by the presence of potash feldspar (Yoder *et al.*, 1957; Luth *et al.*, 1964). Unless the fugacity of water was systematically lower in the granitoid assemblages, they should have melted more extensively than the trondhjemitoid. Evidence supporting this proposition comes from the relatively simple case of a rock containing potash feldspar but no muscovite; this rare occurrence (for the Huntly–Portsoy area) of a *biotite-granitoid* is found on East Head (grid reference 603669). From its grain-size and texture it is judged to be predominantly leucosomatic, but its modal composition is variable and its macroscopic structure diffusely inhomogeneous (nebulitic). Plagioclase composition ranges approximately from An_{20} to An_{40}. This rock is interpreted as the result of pervasive melting of a metasedimentary band that fortuitously had low-melting composition. Such extensive melting is likely to lead to melt compositions departing from cotectic curves. This effect may explain some of the scatter in fig. 9. The replacement textures that affect the amount of potash feldspar and plagioclase in observed assemblages may also have an effect.

The electron-probe data confirm that phenomena in the muscovite-granitoids are very similar to those in the trondhjemitoids. The behaviour of plagioclase compositions is consistent with the melting model. Again, the observation of distinctive plagioclase composition ranges in different neosome pairs indicates control of compositions within localized systems.

The assemblage quartz–plagioclase–microcline–muscovite–sillimanite–biotite. As remarked by Evans and Guidotti (1966), the sub-assemblage quartz–potash-feldspar–muscovite–sillimanite calls for explanation where it occurs over a wide area, as it does

[1] Approximately 10 counts of 10-second duration for Na and Ca were taken at each point. If these showed increase in Ca and decrease in Na from one point to the other, the statistical significance (at 95 % level) of this effect was assessed by applying the standard *t*-test to the counts.

in the present study (fig. 1). In the system K_2O–Al_2O_3–SiO_2–H_2O, the sub-assemblage is univariant in the presence of a gas phase of pure H_2O. The reaction relating the phases is

$$\underset{\text{muscovite}}{K_2Al_4(Si_6Al_2O_{20})(OH)_4}+\underset{\text{quartz}}{2SiO_2} \rightleftharpoons \underset{\text{potash-feldspar}}{2KAlSi_3O_8}+\underset{\text{sillimanite}}{2Al_2SiO_5}+2H_2O \quad (2)$$

a simplified version of the reaction of the sillimanite–potash-feldspar 'isograd' above. Dealing with unmigmatized rocks, Evans and Guidotti (1966) consider only subsolidus reactions, and argue that the Na and Ca content of the natural minerals is insufficient to produce noticeable bivariance (see also Thompson, 1974). Thus, in the presence of all four solid phases in the above equation (2), f_{H_2O} is a function of pressure and temperature only. Where all four phases persist over a wide area, f_{H_2O} must have been *buffered* by the assemblage. This requires that the gas phase, if present, was not pure H_2O. This conclusion also applies to the migmatites under discussion, in which the full assemblage is ubiquitous. It could be argued that the reaction textures in the leucosomes indicate that each rock has an assemblage recording the last temperature of reaction as it cooled; different, adjacent rocks would represent different temperatures. However, persistence of non-reaction muscovite in restites indicates that muscovite (as well as quartz) was present at the thermal climax in almost all cases.

Evans and Guidotti (1966) explain the buffering effect in subsolidus assemblages by proposing that H_2O, generated by dehydration of muscovite with quartz, entered an impure gas phase and failed to escape freely from the rocks. In the Huntly–Portsoy migmatites, on the other hand, a melt is held to have been present. In K_2O–Al_2O_3–SiO_2–H_2O, the muscovite–quartz reaction in the presence of a melt is

$$\text{muscovite}+\text{quartz} \rightleftharpoons \text{potash-feldspar}+Al_2SiO_5+\text{melt} \quad (3)$$

which is shown as the reaction [V] in fig. 10, where reaction (2) is represented as [L]. In the case of reaction (3), 'impurities' imparting bivariance, and so permitting f_{H_2O} to be buffered, must reside in the melt. A gas phase that is not pure H_2O may be present, but the 'impurities' in it could produce noticeable bivariance only if they are also highly soluble in the melt. A more obvious source of additional components in the melt is plagioclase. That the depression of reaction temperatures by the addition of Na_2O, introducing the phase albite, is greater for reaction (3) than for (2) is shown by the calculations of Thompson (1974). Where CaO is also present, it will be partitioned between coexisting melt and plagioclase over a wide temperature interval, over much of which it will be possible for muscovite and quartz to persist with sillimanite and potash feldspar, thus buffering f_{H_2O}. At given pressure and temperature, the melt composition is then a function of initial plagioclase composition, an effect which is probably responsible for much of the scatter in fig. 9. A minor contribution to variability of melt composition, and hence to the temperature range over which buffering is possible, may be made by accessory minerals, not involved in the subsolidus reactions, which participate in melting. A likely example of such a 'fluxing' accessory in the Huntly–Portsoy rocks is tourmaline. In the migmatites, this is strongly concentrated in coarse leucosomes of almost pegmatitic grain-size, suggesting late crystallization during the retrograde evolution of the melts.

Persistence of the full muscovite-bearing assemblage in the migmatites is, then, attributed to bivariance, permitted by the presence in the melt of components which would not be important constituents of a gas phase. This enabled the fugacity of water to be buffered by the solids. If a gas was present, it was not pure H_2O. Buffering of f_{H_2O} by a dehydration reaction in the presence of a multicomponent melt is discussed in a more general context by Fyfe (1970).

Discussion. The petrography of the muscovite-granitoid migmatites is explained by a series of reactions analogous to those shown, for the simplified system K_2O–Al_2O_3–SiO_2–H_2O, at pressures above the invariant point on fig. 10. As temperatures increased, rocks initially containing two feldspars incipiently melted by the 'granite minimum' reaction quartz+plagioclase+potash-feldspar+accessories+vapour $\rightleftharpoons$ melt. However, such rocks are uncommon in the area, being best represented by the 'biotite-granitoid' nebulite.

Rocks with muscovite but initially lacking potash feldspar melted incipiently at higher temperature, by the reaction quartz+plagioclase+muscovite+accessories+vapour $\rightleftharpoons$ sillimanite+melt.

Advanced melting, producing most of the observed leucosomes, was initiated by onset of the reaction:

$$\text{muscovite}+\text{quartz}+\text{plagioclase} \rightleftharpoons \text{potash-feldspar}+\text{sillimanite}+\text{melt}. \qquad (4)$$

This reaction proceeded gradually over a temperature interval, as fugacity of water declined in the multicomponent melt. It rarely went to completion; fugacity of water and the extent of melting were controlled by (4) in most rocks at the climax.[1]

The retrograde reaction textures in the leucosomes are held to have formed in the presence of melt, by the retrograde version of reaction (4). Thus, the 'fluid' of equation (1) was the melt. Presence of this fluid in relatively large bulk facilitated the exchange reactions, between fluid and feldspar, invoked by Ashworth (1972, 1973) for the genesis of the myrmekite in the replacement aggregates. Reaction (1) usually failed to go to completion: failure of rehydration of sillimanite–potash-feldspar would leave relatively large concentrations of water in those parts of the leucosomes that were last to crystallize, and this enrichment in water is probably responsible for the presence of coarse tourmaline-bearing pegmatitic patches. One might speculate that some of the late pegmatite dykes of the area (Read, 1923) might represent the mobile residua of the migmatization event, but an alternative hypothesis is that they may be related to the Newer Granite intrusions, which are much younger than the migmatization (Pankhurst, 1974).

[1] The proportions of the phases involved in a univariant model for reaction (4) can be quantified if the phase compositions are estimated. To a first approximation, the reaction can be modelled in the system Na_2O–K_2O–Al_2O_3–SiO_2–H_2O with the melt assumed to have a typically granitic composition, by weight 0·26 Qz, 0·21 Or, 0·48 Ab, and 0·05 H_2O.

This melt composition in molar terms is 0·45 Qz, 0·08 Or, 0·19 Ab, and 0·29 H_2O. Using typical observed muscovite and potash-feldspar compositions (*cf.* Ashworth, 1972, 1975), the model reaction is then $0{\cdot}14K_{1{\cdot}88}Na_{0{\cdot}12}Al_4(Si_6Al_2O_{20})(OH)_4+0{\cdot}73SiO_2+0{\cdot}22NaAlSi_3O_8 \rightarrow 0{\cdot}29Al_2SiO_5+0{\cdot}24K_{0{\cdot}8}Na_{0{\cdot}2}AlSi_3O_8+1$ melt. In volume terms, there is approximately twice as much potash-feldspar as sillimanite in the residue, despite the generation of melt with a high concentration of feldspar components. This rough calculation explains the observed commonness of potash feldspar in restites.

The reaction textures enabled reaction (4) to be identified in the muscovite-granitoids. Similar textures enable a sequence of reactions at higher grades to be established in the next section.

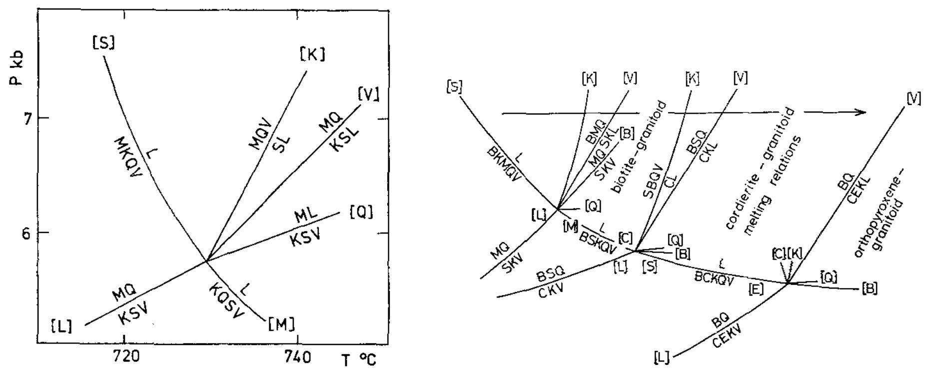

FIGS. 10 and 11: FIG. 10 (left). *P–T* diagram of relevant univariant reactions in the system $K_2O–Al_2O_3–SiO_2–H_2O$ according to recent experimental investigations, after Huang and Wyllie (1974, fig. 3). Notation: K = potash-feldspar, L = melt, M = muscovite, Q = quartz, S = sillimanite, V = aqueous gas phase. A letter in brackets indicates the phase absent from a univariant reaction. FIG. 11 (right). Schreinemakers' model illustrating the proposed reaction scheme from lowest to highest grades of granitoid migmatization in the Huntly–Portsoy area, as modelled in the system $K_2O–Al_2O_3–MgO–SiO_2–H_2O$. Pressure increases upwards; temperature increases from left to right. Notation: B = biotite (eastonite), C = cordierite, E = orthopyroxene (enstatite), K = potash feldspar, L = melt, M = muscovite, Q = quartz, S = sillimanite, V = aqueous gas phase. A letter in brackets identifies the phase absent on a univariant line emanating from a 7-phase invariant point. Horizontal arrow indicates the sequence of grades inferred in the Huntly–Portsoy rocks.

Aspects of the cordierite-bearing migmatites

These migmatites are much more complex, mineralogically and texturally, than the lower-grade ones. Their treatment here will be purely petrographic. The aim of this section is to show that they represent high-grade phenomena complementary to the lower-grade effects already described.

Petrography. The petrographic distinction between leucosomes and restites remains valid, but the only easily observable and constant difference between the two is in grain-size. Modal complexity, with several additional major minerals in leucosomes (notably cordierite, garnet, and orthopyroxene) hinders compositional characterization, though restites tend to be oligomineralic. It is also impossible to illustrate 'typical' textures. Almost all pelites, semipelites, and psammites at these grades are migmatized: palaeosomes consist mostly of highly calcareous lithologies.

The characteristic sub-assemblage of the *cordierite-granitoids* is quartz–plagioclase–potash-feldspar–cordierite–biotite. Sillimanite and garnet usually occur in addition. Biotite is red-brown as in the other migmatites. Sillimanite is usually acicular, but less fine-grained than in the muscovite-granitoids. Potash feldspar rarely shows microcline twinning, and is generally referable to orthoclase. Plagioclase is similar to that of the muscovite-granitoids, but more often complexly zoned. The garnet is almandine, which is often much coarser than the other minerals and is often clearly associated with leucosomes rather than restites. Staurolite and spinel are scarce and fine-grained, the latter confined to restites and almost invariably surrounded by aggregates of cordierite. Opaque minerals are more conspicuous than in the lower-grade migmatites; ilmenite, pyrite, pyrrhotine, chalcopyrite, and graphite were identified. Pyrrhotine is usually altered.

The coarse, leucosome-dominated muscovite-cordierite-granitoids present an extreme structural contrast with the hornfelses that succeed them at higher grade, but their mineralogy is similar, consisting of quartz–plagioclase–potash-feldspar–muscovite–cordierite–garnet–sillimanite–biotite plus opaques and other accessories. Whereas cordierite in the hornfelses is usually pristine, that in the muscovitics is usually altered to nearly isotropic yellow or green material, or to pinite. These late alteration effects are distinct from the reaction textures described below.

The characteristic sub-assemblage of the *noritoids* is quartz–plagioclase–hypersthene–cordierite–garnet–biotite. Biotite and garnet are like those of the other migmatites. Plagioclase ranges up to relatively calcic composition (An_{77}). It is strongly zoned in leucosomes; zoning is often complex but generally trends in the normal sense .The orthopyroxene shows faint pink-green pleochroism. Cordierite is usually unaltered. Spinel and the same opaque minerals as in the cordierite-granitoids were identified. Cummingtonite is scarce, and there is a little orthoamphibole, mostly as reaction rims around orthopyroxene. Two noritoid leucosomes were observed to contain sillimanite, but only as isolated clots completely enclosed in cordierite. In the Huntly–Portsoy area, it can be concluded, sillimanite was incompatible with orthopyroxene. Potash feldspar occurs with orthopyroxene only at a few localities near the centres of the large Basic Masses (*cf.* Read, 1923, pp. 144–6). The interpretation of joint occurrences in leucosomes is problematic because the textures are such that the orthoclase could have crystallized relatively late, after the orthopyroxene had been removed from contact with the melt by armouring. Contacts between orthopyroxene and orthoclase occur without indications of reaction in a few non-leucosomes, but at least one of these is a calcareous palaeosome, so that low content of water probably contributed to the production of the anhydrous paragenesis.

Reaction textures are distinguished from later alteration of, for example, cordierite by the same features that indicate an early origin for the reaction textures in the muscovite-granitoids; the minerals involved are those of the main assemblage, and biotite is the same colour as that in the rest of the rock. Moreover, the reaction aggregates cannot be spatially demarcated precisely, but merge into the general texture of the rock (cf. Ashworth, 1972, 1973).

Cordierite is often rimmed or replaced by aggregates of sillimanite and biotite, sometimes with quartz. In one case, potash feldspar is seen to be rimmed by biotite and quartz. Myrmekite in the cordierite-bearing migmatites is mostly of the type attributable to exsolution (Ashworth, 1972), but occurs in the absence of potash feldspar in one rock having also the cordierite-replacement texture, which suggests a reaction exit of potash feldspar analogous to that in the muscovite suite. In one noritoid showing retrograde evolution to a muscovite-granitoid condition, garnet is partly replaced by biotite and quartz. Orthopyroxene usually reacts to either orthoamphibole, or biotite–quartz (in one case accompanied by cordierite).

Interpretation. If the melting model for the lower-grade migmatites is correct, the higher-grade rocks must have been within the melting range, and since they are migmatized it will be assumed that the reactions occurred in the presence of melt. The aim is to pursue the supersolidus reaction sequence to higher grades than those already discussed. The indications of the retrograde reaction textures are:

cordierite$\pm$potash feldspar+melt$\rightarrow$sillimanite+biotite+quartz

garnet+melt$\rightarrow$biotite+quartz

orthopyroxene+melt$\rightarrow$orthoamphibole

orthopyroxene+melt$\rightarrow$biotite+quartz$\pm$cordierite.

Other phases, such as plagioclase, presumably participated, but are not conspicuous petrographically. Because of the variable compositions of most of the phases, these reactions are presumably at least bivariant. Biotite is evidently a key mineral. Since biotite assemblages in general break down at higher temperatures than muscovite ones (*cf.* e.g. Brown and Fyfe, 1970), and since biotite is the major hydrous mineral remaining in the rocks of semipelitic derivation after muscovite has been consumed, biotite reactions are the most important ones at high grade.

In the absence of directly applicable experimental work, these reactions are here modelled by the method of Schreinemakers (Zen, 1966), giving the schematic model shown in fig. 11, in the system K_2O–Al_2O_3–MgO–SiO_2–H_2O. The sequence of reactions corresponds closely to a part of the scheme erected independently by Grant (1973), who tentatively attempts some quantification of pressure and temperature coordinates. In his nomenclature, the present assemblages are facies-type IV. This is consistent with his placing of the orthoamphibole–orthopyroxene transition (Grant, 1973, fig. 3A).

Presence of plagioclase will render all the reactions at least bivariant, and presence of FeO allows garnet to enter the reaction scheme (Grant, 1973). TiO_2 will not change the variance in the presence of ilmenite, but will affect the phase compositions somewhat.

Multivariance of the reactions in the presence of a large number of components explains the spatial overlap between muscovite-granitoid and cordierite-granitoid parageneses. Furthermore, there is evidence of additional reactions involving fewer phases than those reactions modelled in fig. 11. Most obviously, there is the cordierite-noritoid melting reaction biotite+quartz$\pm$cordierite+plagioclase $\rightleftharpoons$ orthopyroxene+melt, whose temperature field evidently overlaps with that of the cordierite-granitoids. Further reactions in noritoids are discussed by Gribble (1968, especially fig. 5). At slightly lower grade, frequent textural indications of replacement of cordierite without apparent reaction of potash feldspar suggest a continuous reaction such as cordierite+melt $\rightleftharpoons$ biotite+sillimanite+quartz+plagioclase.

At high grade, fig. 11 shows a reaction ushering in compatibility of the pair orthopyroxene–orthoclase (cf. Grant, 1973), leading to orthopyroxene-granitoid (charnockitoid?) migmatites. The rarity and anomalous nature of orthopyroxene–orthoclase coexistences in the Huntly–Portsoy area indicate that this reaction marks the upper limit of grade attained in the area.

Grade increases systematically towards and within the Newer Basic Masses. Intensity of migmatization appears to increase less regularly. The transition from muscovite-granitoid to cordierite-granitoid assemblages is at first accompanied by increasing prominence of leucosomes, but in the high-grade cordierite-granitoid migmatitic hornfelses found at the edges of Newer Basic outcrops, leucosomes are smaller and less coarse. This is attributed to early dehydration of the bulk rock-systems by the adjacent, highly water-undersaturated basic magma. Within the Newer Basic Masses, where metasedimentary inclusions suffered sustained heating, migmatization is again obvious despite the undoubted occurrence of bulk dehydration. Noritoids, which are confined to localities within the Basic Masses, represent wholesale melting, even of relatively calcareous lithologies.

Conclusions

The migmatites of the Huntly–Portsoy area exhibit a range of assemblages from low to high grade within the Sillimanite–potash-feldspar Zone. The lowest grade is characterized by the occurrence of trondhjemitoid and muscovite-granitoid migmatites. In the trondhjemitoids, which lack potash feldspar and are not complicated by reaction textures, the cotectic compositions of leucosomes, together with their textural immaturity and plagioclase zoning, lead to the conclusion that the leucosomes crystallized from melts. Correlation between leucosome and melanosome plagioclase compositions, and the persistence of sodic palaeosomes, point to origin of the melts within small closed systems. The leucosomes are thus interpreted as melt-mobilizates, and the melanosomes as complementary restites. The initial water content of a rock-system controlled the extent of melting. Water-undersaturation may have contributed to the evolution of plagioclase compositions as the melt crystallized.

The muscovite-granitoid migmatites are attributed to the same process of partial melting. The main melting reaction involved partial dehydration of the pair muscovite–quartz. The compositionally complex melt phase is believed to have allowed buffering of the fugacity of water, by this reaction, within small closed systems.

Retrograde crystallization of the melt produced replacement textures in which potash feldspar and sillimanite are partly replaced by the hydrous equivalent, muscovite–quartz–plagioclase. Retrograde reactions were inevitable in the presence of melt. The textures permit identification of the sequence of major melting reactions with increasing grade in this area. Partial dehydration of biotite–sillimanite–quartz produced cordierite–orthoclase, and partial dehydration of biotite–quartz in the absence of sillimanite and potash feldspar produced orthopyroxene. Sillimanite is incompatible with orthopyroxene in the assemblages of this area, and orthopyroxene is incompatible with orthoclase except at the most extreme grade, seen in only a few localities.

The Huntly–Portsoy area is fortunate in having a variety of well-preserved migmatites. Late-orogenic deep-seated intrusion of basic magma produced a range of grades within a small area. Subsequent cooling was rapid enough to prevent complete equilibration, and there was little later orogenic activity. The area presents an interesting example of localized but pervasive migmatization in a marginally orogenic setting. Although the difficulties will often be greater in other areas, it is hoped that the description of these relatively easily interpretable rocks will be of assistance to other petrologists working on migmatites.

Acknowledgements. This work was done while I was a NERC-supported research student at the Department of Mineralogy and Petrology, Cambridge. It was supervised by Dr. S. O. Agrell, and by Dr. G. A. Chinner, whose serendipity in selecting the area merits commemoration. I am indebted to Dr. S. W. Richardson for subsequent advice.

REFERENCES

ASHWORTH (J. R.), 1972. *Geol. Mag.* **109**, 45–62.
—— 1973. Ibid. **110**, 77–80.
—— 1975. Ibid. **112**, 113–36.
BROWN (G. C.), 1970. *Earth Planet. Sci. Letters*, **9**, 355–8.
—— and FYFE (W. S.), 1970. *Contr. Min. Petr.* **28**, 310–18.
CHINNER (G. A.), 1966. *Quart. Journ. Geol. Soc.* **122**, 159–86.
DEER (W. A.), HOWIE (R. A.), and ZUSSMAN (J.), 1963. *Rock-forming Minerals*, **4**. London (Longmans).
DEVORE (G. W.), 1956. *Journ. Geol.* **64**, 31–55.
EVANS (B. W.) and GUIDOTTI (C. V.), 1966. *Contr. Min. Petr.* **12**, 25–62.
FLINN (D.), 1969. *Lithos*, **3**, 361–70.
FYFE (W. S.), 1970. In *Mechanism of Igneous Intrusion* (G. NEWALL and N. RAST, editors). Liverpool Geological Society.
GRANT (J. A.), 1973. *Amer. Journ. Sci.* **273**, 289–317.
GRIBBLE (C. D.), 1968. *Contr. Min. Petr.* **17**, 315–30.
—— 1970. *Scot. Journ. Geol.* **6**, 75–82.
HUANG (W. L.) and WYLLIE (P. J.), 1974. *Amer. Journ. Sci.* **274**, 378–95.
KALSBEEK (F.), 1970. *Medd. Grønland*, **189**, part 1.
KRETZ (R.), 1969. *Lithos*, **2**, 39–66.
LOBERG (B.), 1963. *Geol. För. Förh.* **85**, 3–109.
LUTH (W. C.), JAHNS (R. H.), and TUTTLE (O. F.), 1964. *Journ. Geophys. Res.* **69**, 759–73.
MEHNERT (K. R.), 1953. *Neues Jahrb. Min., Abh.* **85**, 59–140.
—— 1957. Ibid. **90**, 39–90.
—— 1962. Ibid. **98**, 208–49.
—— 1963. Ibid. **99**, 161–99.
—— 1968. *Migmatites and the Origin of Granitic Rocks.* Amsterdam (Elsevier).
MISCH (P.), 1968. *Contr. Min. Petr.* **17**, 1–70.
PANKHURST (R. J.), 1974. *Geol. Soc. Amer. Bull.* **85**, 345–50.
READ (H. H.), 1923. *The Geology of the Country around Banff, Huntly and Turriff.* Memoir of the Geological Survey of Scotland, for sheets 86 and 96.
—— 1927. *Trans. Roy. Soc. Edin.* **55**, 317–54.
—— 1943. *Proc. Geol. Assoc.* **54**, 64–85.
—— 1952. *Trans. Edin. Geol. Soc.* **15**, 265–79.
THOMPSON (A. B.), 1974. *Contr. Min. Petr.* **44**, 173–94.
TURNER (F. J.), 1968. *Metamorphic Petrology: Mineralogical and Field Aspects.* New York (McGraw-Hill).
VAN DER PLAS (L.), and TOBI (A. C.), 1965. *Amer. Journ. Sci.* **263**, 87–90.
WINKLER (H. G. F.), 1967. *Petrogenesis of Metamorphic Rocks*, 2nd edn. New York (Springer-Verlag).
YODER (H. S., *Jr.*), 1967. *Carnegie Inst. Washington Yearbook* **66**, 477–8.
—— STEWART (D. B.) and SMITH (J. R.), 1957. Ibid. **56**, 206–14.
ZEN (E-AN), 1966. *U.S. Geol. Surv. Bull.* **1225**.

[*Manuscript received 4 November 1974, revised 12 September 1975*]